Functional connectivity alterations of the temporal lobe and hippocampus in semantic dementia and Alzheimer's disease

Simon Schwab[1], Soroosh Afyouni[1] , Yan Chen[2], Zaizhu Han[3], Qihao Guo[3], Thomas Dierks[4], Lars-Olof Wahlund[5], and Matthias Grieder[4]

1 Big Data Institute, Li Ka Shing Centre for Health Information and Discovery, Nuffield Department of Population Health, University of Oxford, Oxford, United Kingdom
2 State Key Laboratory of Cognitive Neuroscience and Learning, Beijing Normal University, Beijing, China
3 Department of Neurology, Huashan Hospital, Fudan University, Shanghai, China
4 Translational Research Center, University Hospital of Psychiatry, University of Bern, Bern, Switzerland
5 Karolinska Institute, Department NVS, Division of Clinical Geriatrics, Stockholm, Sweden

Corresponding author: Matthias Grieder, PhD, Translational Research Center, University Hospital of Psychiatry Bern, Bolligenstrasse 111, 3000 Bern 60, Switzerland. Tel.: +41 319328351; Fax: +41 319309961; E-mail: matthias.grieder@upd.unibe.ch

Abstract

The temporal lobe is a central core of neurodegeneration in Alzheimer's disease and semantic dementia. The severe semantic memory impairments in semantic dementia have been attributed to their pronounced anterior temporal lobe atrophy and functional disruption. In contrast, medial and posterior temporal lobe damage predominantly found in patients with Alzheimer's disease has been associated with episodic memory disturbance. Despite these seemingly distinct neuropathological signatures that correspond well to the syndrome-typical symptomatology, hippocampal deterioration common in Alzheimer's disease and semantic dementia appears paradoxical. In attempting to gain more insight into mutual and divergent functional alterations of Alzheimer's disease and semantic dementia, we assessed intrinsic functional connectivity between temporal lobe regions in patients with Alzheimer's disease (n = 16), semantic dementia (n = 23), and healthy controls (n = 17). Other than the majority of studies that conducted comparable analyses, we were particularly interested in connectivity alterations between functional rather than anatomical regions, and therefore used a functional parcellation of the temporal cortex. Unexpectedly, the Alzheimer's disease group showed only a single connection with reduced functional connectivity as compared to the controls. It was comprised of the right orbitofrontal cortex and the right anterior temporal lobe. In contrast, functional connectivity was decreased in the semantic dementia group in six connections, mainly involving hippocampus, lingual gyrus, temporal pole, and orbitofrontal cortex. In our view, the relatively intact functional connectivity in the Alzheimer's disease sample was owed to their relative mild state of the disease. Nevertheless, we identified a common pathway with semantic dementia, since functional connectivity between right anterior temporal lobe and right orbitofrontal cortex was reduced in both dementia types. This might be related to impairments in social behavior frequently observed in patients. Moreover, besides the expected functional connectivity disruptions in brain regions associated with language processing and semantic memory, our results point to the importance of an intact anterior temporal lobe for a sound semantic and social functioning.

Introduction

Everybody occasionally experiences difficulties in integrating past events into an accurate context — a condition classified as an episodic memory disturbance. Episodic memory functioning requires the processing of information about chronology, place and the protagonists who were involved in an event. The capability of storing and retrieving autobiographical memory instances is however not sufficient for an intact episodic memory: we also strongly rely on a fully functioning semantic memory. Concretely, semantic memory reflects our general knowledge about concepts such as objects, people, and words. Thus, only a sound interplay of these two memory systems, episodic and semantic memory, allows a cognitively healthy state of an individual.

Some time ago, two initially contradicting models of the neurophysiological organization of the semantic memory have been harmonized as what can be characterized as a 'cortically distributed plus semantic hub' theory (Mummery et al., 2000; Guo et al., 2013). Distributed refers to the idea that regions that process semantic concepts receive multimodal input from corresponding brain regions (e.g. visual attributes from visual brain regions, tactile attributes from the sensorimotor cortex, etc.). In the semantic hub, these multimodal inputs from distributed cortical areas converge to so-called unitary semantic concepts (McClelland and Rogers, 2003; Patterson et al., 2007). The semantic hub was found to be localized in the anterior temporal lobe bilaterally, a region which is atrophied or hypometabolized in patients with the semantic variant of PPA, also known as the temporal variant of frontotemporal dementia (FTD) or semantic dementia (SD) (Hodges and Patterson, 2007; Patterson et al., 2007; Landin-Romero et al., 2016). In SD, the onset of grey matter atrophy occurs in the anterior temporal lobes, frequently with an asymmetry towards the more affected left hemisphere. With progression of the disease, temporal pole, medial and lateral temporal areas are degenerated. However, the patients seem to exhibit an almost intact episodic memory, while the semantic memory is severely deteriorated.

In contrast to SD, patients with Alzheimer's disease (AD) show predominantly episodic memory impairments, and semantic memory deficits can only be observed to a lower degree (Blackwell et al., 2004; Vogel et al., 2005; Mascali et al., 2018). AD has been described as a disconnection syndrome, that is, connections of functionally or structurally linked brain regions that are part of a network become increasingly disrupted (Seeley et al., 2009; Villain et al., 2010; Wang et al., 2013). This degenerative mechanism has been associated with the cognitive deficits of patients with AD (Reijmer et al., 2013; Tijms et al., 2014; Liu et al., 2016). A common finding in AD is that grey matter atrophy onset can be localized in hippocampal, entorhinal, and parietal brain regions. The hippocampus is a core region for episodic memory encoding. However, it has also been associated with semantic memory functions (Burianova et al., 2010). In fact, Burianova and colleagues (2010) postulated that the hippocampus is part of a common declarative memory network (i.e. semantic and episodic/autobiographical memory).

The existence, spatial patterns, or other properties of a functional network, as for example Burianova and colleagues' proposed declarative memory network, are commonly assessed by the use of a functional connectivity (FC) analysis. The simplest, yet most straightforward interpretable approach to quantify FC is to compute the temporal correlation between seed regions. Seed regions are a priori selected brain regions upon which the particular research question is investigated. If less or no assumptions are made, data-driven independent component analysis (ICA) or hierarchical approaches can be applied. These latter methods are more sophisticated but also more demanding in terms of interpretation (Fox and Raichle, 2007; Smith et al., 2013). Despite these different analysis strategies, the mutual rationale of FC is that brain regions that demonstrate a statistical dependence are considered functionally connected (Biswal et al., 1995).

This kind of large-scale network analysis has widely been applied to clinical samples such as AD and SD. Accordingly, changes of FC (decreases and increases) in AD often involve the hippocampus (Wang et al., 2006; Allen et al., 2007; Tahmasian et al., 2015). With the progression of the disease, structural and functional connectivity distortions affect several networks, for instance involving particularly the parahippocampus (Brier et al., 2012; Liu et al., 2016). Neuronal loss in SD is found in core regions such as the temporal pole, anterior middle temporal gyrus, inferior temporal gyrus, and insula (Hodges and Patterson, 2007; Ding et al., 2016). Other regions affected by atrophy have been reported and included inferior orbitofrontal gyrus, amygdala, and hippocampus (Agosta et al., 2014). Both structural and FC appear to be deteriorated in regions either affected by or proximate to the core of atrophy (Farb et al., 2013; Agosta et al., 2014; Andreotti et al., 2017). However, reduced FC of the anterior temporal lobe with various cortical regions were also found in SD (Guo et al., 2013). Moreover, Ding et al. (2016) showed that grey matter loss is associated with the cognitive impairments found in SD.

Considering these findings as well as the distinct pathology of AD and SD, the mere neuronal loss of hippocampal cells might not be the sole cause of episodic memory deficits. In other words, it is not a necessity. Similarly, temporal pole atrophy might not be necessary (but is sufficient) to lead to semantic impairment. For instance, La Joie et al. (2014) identified the hippocampus as a 'main crossroad' between brain networks that are disrupted in AD and SD. Despite the growing body of research, the common and divergent changes of FC in the temporal lobes in AD and SD are not fully understood. Moreover, to our best knowledge, the functional reorganization of the disrupted connectome of the semantic memory in SD has not been studied so far. Furthermore, most studies investigating FC used anatomical parcellation to obtain the spatial properties of functional networks. In our view however, it appears to be more reasonable to take advantage of the now available functional atlases for this purpose. Therefore, new insights might be gained by analyzing FC changes in AD and SD based on functionally segregated brain regions.

We aimed at disentangling alterations of FC using a refined division of temporal subregions: sixty-six functional regions of interest (ROIs) from the Craddock atlas overlap with the temporal lobes (Craddock et al., 2012). Other than numerous previous studies, we accounted for structural changes (i.e. grey matter atrophy) in order to provide FC data about the functional reorganization of the temporal lobes affected by

atrophy, while changes of FC merely due to atrophy were of no interest. We investigated the pairwise region-to-region FC between each of the 66 ROIs in three participant groups (AD, SD, and healthy elderly controls). We focused our analysis on the temporal lobes with the following rationale: first, brain regions identified as the origin of atrophy are located in the temporal lobe. Second, a 'crossroad' in FC network disruption in AD and SD was found in the hippocampus. Third, functional hubs for episodic and semantic memory can be found in the temporal lobe (as outlined above). Fourth, the strongest FC of temporal regions are located within the temporal lobes and concur with functional networks crucial for language processing, the core clinical feature of SD (Hurley et al., 2015). A common issue with studies involving SD is the small sample size due to the low prevalence and relatively difficult diagnosis. This has led to a knowledge about SD pathology that is based on studies with comparably small sample sizes. In order to overcome this to some extent, we pooled two available data sets from two recording sites (see Method section for details). Orban et al. (2018) showed that it might be advantageous to use multisite fMRI-data and that generalizability appears to be given. However, we will address some limitations of this approach in the Discussion section.

In line with the studies circumscribed above, we tested the following hypotheses: for the AD sample, we expected alterations of FC in hippocampus, parahippocampal regions, and possibly posterior temporal regions. For SD, altered FC could be anticipated in the hippocampus, the fusiform gyrus, and the temporal pole.

Methods

Participants

We analyzed resting-state fMRI data from a total of 62 participants from three groups: semantic dementia (SD), Alzheimer's disease (AD), and a healthy elderly control group (HC). We examined all the functional MR data and excluded six datasets due to insufficient data quality (see data quality control). The final sample consisted of 56 participants: Twenty-three patients with SD, with a mean age (std. dev.) of 62 (7), 16 patients with AD, mean age 68 (9), and 17 individuals in the HC group, mean age 68 (3), see Table 1 for demographic descriptives and clinical scores Patients with SD from the Stockholm site were collected throughout Sweden and diagnosed using the criteria of Neary et al. (1998), while patients with SD from Shanghai were recruited from Huashan Hospital in Shanghai, according to the criteria of Gorno-Tempini et al. (2011). Patients with AD were recruited at the Memory Clinic of the Geriatric Department at Karolinska University Hospital in Huddinge, Sweden. Their diagnosis was performed by expert clinicians and was in accordance with the ICD-10 criteria. The patients with AD included in this study underwent a standard clinical procedure which consisted of examinations such as structural neuroimaging, lumbar puncture, blood analyses, and a neuropsychological assessment. Further inclusion criteria for all patients was a Global Deterioration Scale

lower than 6 (i.e. moderate dementia or milder) and the Cornell Depression Scale below 8. Healthy elderly controls were recruited by advertisement and provided written informed consent prior the data acquisition. Presence of medical or psychiatric disorders (other than dementia), intake of drugs affecting the nervous system, or magnetic implants, led to an exclusion from the study.

MR data

MR images were acquired on two sites: The Karolinska Institute in Stockholm, Sweden, and the Huashan Hospital in Shanghai, China.

Stockholm site

MR images were acquired with a 3T Siemens Magnetom Trio scanner (Siemens AG, Erlangen, Germany). Structural images were 3D T1-weighted magnetization-prepared rapid gradient echo (MPRAGE) images using the following parameters: TR = 1900 ms, TE = 2.57 ms, flip angle = 9°, matrix size = 256 × 256, field of view = 230 × 230 mm^2, slice number = 176 slices, slice thickness = 1 mm, and voxel size = 0.90 × 0.90 × 1 mm^3. The structural images were previously used for voxel-based morphometry and published with a different purpose and sample configuration (Grieder et al., 2013; Andreotti et al., 2017). Functional images were acquired with a 32-channel head coil, using an interleaved EPI sequence (400 volumes; 26 slices; voxel, 3 × 3 × 4 mm^3; gap thickness, 0.2 mm; matrix size, 80 × 80; FOV, 240 × 240 mm^2; TR, 1600 ms; TE, 35 ms).

Shanghai site

Images were acquired with a 3T Siemens Magnetom Verio. Structural images were 3D T1-weighted magnetization-prepared rapid gradient echo (MPRAGE) images using the following parameters: TR = 2300 ms, TE = 2.98 ms, flip angle = 9°, matrix size = 240 × 256, field of view = 240 × 256 mm^2, slice number = 192 slices, slice thickness = 1 mm, and voxel size = 1 × 1 × 1 mm^3. Functional images were acquired with a 32-channel head coil, using an interleaved EPI sequence (200 volumes; 33 slices; voxel, 4 × 4 × 4 mm^3; gap thickness, 0 mm; matrix size, 64 × 64; FOV, 256 × 256 mm^2; TR, 2000 ms; TE, 35 ms, flip angle 90°). The data was previously published with a different sample configuration (SD only sample) in a combined structural and functional study using a hippocampus seed region (Chen et al., 2017), as well as in a structural VBM study (Ding et al., 2016).

Preprocessing

Data quality control

We performed pre-processing using SPM12 (http://www.fil.ion.ucl.ac.uk/spm). We initially set all images' origin to the anterior commissure, and then performed slice-time correction, realignment, coregistration,

normalization to MNI space (2 × 2 × 2 mm^3), and smoothing (FWHM 8 mm). Time-series data was high-pass filtered (1/128 Hz) and we regressed out 14 nuisance parameters (6 movement parameters and its first derivative, white matter, and CSF).

We inspected the spatio-temporal quality of each scan by comparing the slow and fast components of the data using DSE (Dvar, Svar & Evar) decomposition (Afyouni and Nichols, 2018). The DSE technique decomposes the dataset into three main components: fast, which is the squared mean difference; slow, which is the squared mean averages, and Evar, which refers to the sum of squares of the two ends of the time series. Subjects with remarkably high divergence (>75%-tile) between Dvar and Svar components are then removed, as suggested in Afyouni & Nichols (2018). Four subjects with highest divergence (>75%-tile) between Svar and Dvar components were discarded.(1 SD; 3 HC). We further excluded two AD subjects, as more than 20% of their DVARS data-point were found to be corrupted. The remaining subjects were scrubbed as suggested by Power et al. (2012). These corruptions were also confirmed by visual inspection of the framewise displacement time series. Thus, altogether we excluded six dataset (9.6%) due to bad data quality. We re-run the diagnostics on on the final sample and we found no difference between groups regarding these diagnostics (one-way ANOVA, all $p > 0.05$).

Functional connectivity analysis

The selection of an atlas and the identification of nodes is critical in studying FC. We used a functional atlas of 66 nodes of the temporal cortex. The reason to use a functional atlas is that anatomical atlases do not directly map to functional units and contain functionally heterogeneous regions. Instead, the nodes of an atlas should represent functionally homogeneous regions and should further match the functional segregation present at the individual level. The functional parcellation we used is based on resting-state fMRI data which was clustered into spatially coherent regions of homogeneous FC (Craddock et al., 2012) and was evaluated in terms of the generalizability of group level results to the individual. From the 200 nodes, we used a subset of 66 temporal regions that showed at least 5–6% overlap with one of the following temporal structures: the superior temporal (temp.) cortex, the middle temp. cortex, the inferior temp. cortex, the temp. pole, the hippocampus, the parahippocampal cortex, the lingual gyrus, the amygdala, the insular cortex, and the fusiform gyrus; these 66 ROIs are shown in Figure 1. We extracted the mean time-series across these regions, resulting in 66 time-series per subject. To address motion and physiological confounds which are global in nature, we applied global signal regression to the time series (Chang and Glover, 2009; Power et al., 2014). We created a pair-wise correlation matrix and transformed the correlation coefficient to Z scores by Fisher's transformation. We conducted a one-way ANCOVA for each node pair (2145 tests) to test the null hypothesis of no difference between the three groups with age as a covariate. We found 317 significant edges that showed a group effect (uncorrected, $p < 0.05$), and after accounting for multiple comparisons, seven edges showed a significant group effect (FDR corrected, $p < 0.05$).

Results

We analyzed functional connectivity of 56 participants using 66 functional nodes of the temporal cortex and and related subcortical areas (hippocampus and amygdala). Seven connections (FC between node pairs) demonstrated a significant difference between the three group after correcting for multiple comparison (FDR corrected, $p < 0.05$). A detailed characterization and test statistics of these seven connections are shown in Table 2; the Z-values for the significant connections are depicted in Figure 2. We performed post-hoc tests (Tukey HSD) for single comparisons of three groups to investigate the particular group contrasts that drove the significant group effect (Table 3). We found that most differences were related to the SD group with significant changes in all of the seven connections: SD showed lower FC in 6 out of 7 connections compared to HC, and higher FC in one connection (edge no. 2) compared to HC. This higher FC in the SD group was also significantly higher compared to the AD group. The AD group had a lower FC compared to HC in only 1 out of the 7 connections (edge 6). Comparing the two patient groups SD versus AD, we found that SD had significant lower FC in 4 connections (edges 3, 4, 5, 7).

We visualized the connectivity structure and connection strengths, see Figure 3. The SD group generally had much lower connectivity compared to the other two groups. An exception was the stronger contralateral connection between the right lateral inferior occipital cortex and the left posterior superior temporal gyrus (edge no. 2). The AD group showed a lower FC compared to HC between the right middle temporal gyrus and the right frontal orbital cortex (edge no. 6). A common finding in all the three group was that the FC between the right fusiform cortex and the right inferior temporal pole was the strongest (no. 3).

Discussion

In this study, we compared functional connectivity between semantic dementia (SD), Alzheimer's disease (AD) and elderly healthy controls (HC) using a functional parcellation of 66 regions of the temporal cortex and hippocampus (i.e., we investigated at intra-temporal connections and connections with contralateral temporal regions). The overall picture that comes across is that between the majority of the significant nodes, SD demonstrated most strikingly a decrease in FC. The AD group appeared to be situated between HC and SD, while most differences to the HC did not reach significance. To our understanding, the often described disconnections found in AD were elusive in our study, owed to the mild state of our AD group. One reason could be that the remaining grey matter volume in brain regions typically affected by neuronal degeneration was sufficient to maintain an intact FC to remote areas. In other words, the damage found in mild stages might affect the intra-regional processing in local neuronal populations, whereas the inter-regional (i.e. network) FC would be affected with more advanced AD progression (McDonough and

Nashiro, 2014). Future studies will require larger sample sizes to demonstrate smaller changes in FC with respect to mild state impairments.

The most intriguing finding of our study for the SD group was the decreased FC between left hippocampus and left/ right lingual gyri (edges 4 and 5). We might have found a breakdown of these connections, as the FC values were negative in SD, but not in AD and HC. The reason for this interpretation is that, given the global signal regression, a breakdown in FC seems more likely than a genuine negative connectivity. These disruptions are characteristic for the neurophysiological basis of the SD patients' typical symptomatology involving an impaired semantic memory. For instance, Sormaz et al. (2017) recently showed a correlation of FC between left hippocampus and lingual gyrus with topographic memory, and a correlation of semantic memory performance with FC to the intracalcarine cortex, a finding strikingly consistent with our results.

Functional connectivity between left anterior superior/ middle temporal gyrus/ insula and left posterior middle/ superior temporal gyrus was decreased in SD contrasted with HC (edge no. 1). It is important to note that this is the single connection that showed an FC difference between SD and HC exclusively (i.e. a finding specific for the SD-HC group single-comparison while the other group contrasts were not significant). These regions are commonly associated with cross-modal integration (i.e. semantic hub), auditory and language processing, as well as the processing of emotionally relevant context. Hence, this finding might reflect the severe semantic deficits in SD (see BNT, AF, VF scores in Table 1) that are manifested by the loss of conceptual knowledge (Landin-Romero et al., 2016).

The single connection that showed increased FC in SD compared to the other groups (edge no. 2) was between left posterior superior temporal gyrus/ parietal opercular cortex/ planum temporale and the right lateral inferior/ superior occipital cortex. The temporal brain areas that constitute this connection are important for early context integration of acoustically presented words (Shtyrov and Pulvermüller, 2007), lexico-semantic retrieval (Jobard et al., 2003), and are part of a supramodal semantic network (Wirth et al., 2008). The occipital node of this connection subserves visual integration. Thus, an increased FC between these regions might reflect a functional reorganization that is characterized by supporting language comprehension using more sensory inputs. Moreover, this result indicated a reduced hemispheric functional specialization and perhaps an attempt to pool resources that are spared.

In comparison with AD and HC, SD patients showed lower FC between the functional ROI encompassing the right fusiform/ parahippocampal gyri and the right inferior temporal pole. Disruption of this connection (no. 3) can be viewed as SD-typical, as the functional profile of the involved regions conforms to SD symptomatology. In particular, the right temporal pole is crucial for single word comprehension and object recognition, which are the hallmark impairments in SD associated with the loss of semantic knowledge (Mesulam et al., 2015; Nilakantan et al., 2017). Moreover, deteriorated right temporal pole integrity plays a role in the social cognitive and behavioral changes observed in SD (Kumfor et al., 2016). The right fusiform gyrus on the other hand is associated with working memory for faces and face perception (Rangarajan et al., 2014; Brunyé et al., 2017), and the right parahippocampal gyrus with working memory for object location as well as episodic buffer (Owen et al., 1996; Luck et al., 2010). Hence, this SD-specific

FC-alteration matched extraordinarily well the well-circumscribed symptomatology of SD (Landin-Romero et al., 2016).

Similar to connection no. 3, FC was reduced in SD compared with AD and HC between the ROI comprised of left lingual/ intracalcarine/ precuneous cortex and the ROI including left hippocampus/ thalamus (connection no. 4). This finding is in line with Seeley et al. (2009), who reported the medial temporal lobe as part of an SD-vulnerable network. Thus, we additionally showed a possible contribution of primary visual (intracalcarine cortex), visual memory (lingual gyrus) and self-awareness (precuneus, i.e. default mode network) regions to that semantic network. It might appear surprising that the FC of the AD group was not significantly reduced in this connection, despite the commonly known medial temporal lobe atrophy and the pivotal role of the hippocampus in episodic memory encoding (Tondelli et al., 2012; La Joie et al., 2014). However, functional and anatomical changes do not necessarily overlap, and for instance, stable FC of left hippocampus in early AD (except with right lateral prefrontal cortex) has been reported previously (Wang et al., 2006).

Lower FC in SD than AD (and HC) was also found between right lingual/ intracalcarine cortex and left hippocampus/ thalamus (connection no. 5). Therefore, connections between bilateral lingual gyri and the left hippocampus were detected in our HC sample (for illustration, see Figure 3, connections no. 4 and 5), whereas either of them were damaged in SD, but not in AD. This supports recent indication of a hippocampal contribution to the semantic memory network (La Joie et al., 2014). Because episodic memory is relatively spared in SD, the connections between left hippocampus and bilateral lingual gyri might contribute to the semantic memory network. On the other hand, we did not find an expected decrease of FC in connection no. 4 in AD, although precuneus and hippocampus contribute to episodic memory, which is impaired in AD. However, we have to bear in mind that our analysis was restricted to temporal lobe FC and thus did not cover the entire episodic memory network including brain regions located in frontal and parietal lobes. Future studies should investigate additional nodes from the aforementioned areas using larger sample sizes to tackle the increased number of connections and multiple testing correction that are associated with larger networks.

The only FC reduction common in both SD and AD compared with HC was found in connection no. 6. The functional role of the involved regions suggests an association with a frequently observed clinical presentation of AD and SD characterized by apathy and agitation associated with the right orbitofrontal cortex (Bruen et al., 2008; Fernández-Matarrubia et al., 2018), and impairments in social cognition and behaviour related to the right anterior temporal lobe (Kumfor et al., 2016). Hence, we added a common pathway to the crossroad described by La Joie et al. (2014). They suggested that the hippocampus is a converging hub of an (AD-affected) episodic and a (SD-affected) semantic network. Accordingly, our data indicated that besides a shared damaged hub in AD and SD, the functional connection between the right anterior middle/ superior temporal gyri and the right orbitofrontal cortex might be a second candidate for the neuropathology shared in both clinical populations.

The final significant connection (no. 7) of the present study was found between left orbitofrontal cortex and left anterior inferior and middle temporal gyri. Literature suggests a functional role of this connection in deficient socioemotional abilities that are found predominantly in the behavioral variant of FTD (Dermody et al., 2016), and in higher level object representation, involving language and auditory processing. Unlike in connection no. 6, the AD group did not show an impaired FC of orbitofrontal regions with the ipsilateral temporal cortex. Thus, one might speculate about a bilateral breakdown of orbitofrontal to temporal connections in SD, which might be a precondition for the manifestation of a semantic deficit.

We also want to address some limitation of our study. Even though the overall sample size is large, the sample sizes of the three subgroup are considered small (16–23 individuals). Larger studies need to be performed, however, this is especially challenging for SD given the low prevalence. Therefore, we pooled two SD samples from two different sites with different scanners; most individuals of the SD group were from a the Shanghai site. The data from different sites may have different noise levels such as thermal noise, physiological noise, and motion (Birn, 2012; Power et al., 2014). These artefacts are global in nature, and global signal regression (GRS) can successfully remove these and not only standardizes the data between sites, but also across individuals. That means the distribution of correlation coefficients is shifted from predominantly positive to mean zero with positive and negative coefficients. The negative correlations can appear as significant anti-correlations and need to be interpreted with caution, however, GRS can also improve the specificity of positive correlations (Murphy and Fox, 2017). Importantly, in this study, we do not interpret absolute negative correlations and solely compare relative differences in correlations between groups.

To summarize the main findings of the current study, the cohort of patients with SD yielded a number of distinct ipsilateral and contralateral connections of the temporal lobe that showed a significant reduction in FC. These connections included the regions on which our predictions were based on (i.e. hippocampus, fusiform gyrus, and temporal pole). Two functional connections were intriguing due to their distinctiveness from the other groups: the first was the connectivity breakdown between left hippocampus and bilateral lingual gyri likely reflecting the neuronal underpinning of semantic memory loss. Secondly, a bilateral disruption of connectivity between temporal and frontal lobes was found. This aligns well to the pathophysiology within the FTD spectrum and especially to semantic and social deficits in SD.

FC in AD was relatively intact compared to SD, which contradicted our hypothesis. The only connection with significantly reduced FC encompassed the right orbitofrontal cortex and the right anterior temporal lobe (no. 6), which we identified as an AD/SD-common pathway. Additionally, Figure 2 illustrates that our AD group had lower FC than HC in connections no. 1, 2, and to a smaller extent no. 5 which all missed significance. These FC signatures in the AD group could be attributed to their mild stage of symptom progression (MMSE of 24.5), and potentially an early marker of the disease, but larger and longitudinal studies are needed.

Following the "cortically distributed plus semantic hub" theory, several connections found significantly altered in the present study affected anterior temporal lobe – semantic hub – regions (no. 1, 3, 6, and 7).

Moreover, their counterparts were partly localized in the modality-specific regions described by Patterson et al. (2007), but also in orbitofrontal regions. On one hand, this convergence of our results with the arguments in Patterson et al. (2007) supported the "distributed plus hub" theory, because we found altered FC in connections between the hub and the modality-specific regions. On the other hand, our findings indicated a relationship of the disturbed semantic memory network with secondary symptoms circumscribed as impaired socioemotional behavior, including apathy and agitation. Thus, an intact FC of the semantic hub appears to be crucial for semantic memory abilities as well as for social competence, for instance.

Taken together, the present study particularly contributed to the understanding of distinct pathophysiological changes in AD and SD that are related to disruptions of functional networks in the temporal lobe. The unique aspect we introduced was the definition of ROIs based on functional brain segregation (rather than anatomy) for FC analysis. Due to the comparably strict statistical approach and the predefined choice of ROIs, our study provided a fine-grained overview of FC aberration related to temporal lobe function in AD and SD.

Data Availability

Data can be requested from the corresponding author. Analysis scripts to generate all results and figures is available from https://github.com/schw4b/ADSD.

Funding

This work was supported by the Swedish Alzheimerfonden, the Swiss Synapsis Foundation, and the University of Bern, and the Beijing Natural Science Foundation (7182088). Simon Schwab acknowledges funding from the Swiss National Science Foundation (SNSF, No. 162066 and 171598).

References

Afyouni S, Nichols TE. 2018. Insight and inference for DVARS. Neuroimage 172:291–312.

Agosta F, Galantucci S, Valsasina P, Canu E, Meani A, Marcone A, Magnani G, Falini A, Comi G, Filippi M. 2014. Disrupted brain connectome in semantic variant of primary progressive aphasia. Neurobiol Aging 35:2646–2655.

Allen G, Barnard H, McColl R, Hester AL, Fields JA, Weiner MF, Ringe WK, Lipton AM, Brooker M, McDonald E, Rubin CD, Cullum CM. 2007. Reduced hippocampal functional connectivity in Alzheimer disease. Arch Neurol 64:1482–1487.

Andreotti J, Dierks T, Wahlund L-O, Grieder M. 2017. Diverging Progression of Network Disruption and Atrophy in Alzheimer's Disease and Semantic Dementia. J Alzheimers Dis 55:981–993.

Birn RM. 2012. The role of physiological noise in resting-state functional connectivity. Neuroimage 62:864–870.

Biswal B, Yetkin FZ, Haughton VM, Hyde JS. 1995. Functional connectivity in the motor cortex of resting human brain using echo-planar MRI. Magn Reson Med 34:537–541.

Blackwell AD, Sahakian BJ, Vesey R, Semple JM, Robbins TW, Hodges JR. 2004. Detecting dementia: novel neuropsychological markers of preclinical Alzheimer's disease. Dement Geriatr Cogn Disord 17:42–48.

Brier MR, Thomas JB, Snyder AZ, Benzinger TL, Zhang D, Raichle ME, Holtzman DM, Morris JC, Ances BM. 2012. Loss of intranetwork and internetwork resting state functional connections with Alzheimer's disease progression. J Neurosci 32:8890–8899.

Bruen PD, McGeown WJ, Shanks MF, Venneri A. 2008. Neuroanatomical correlates of neuropsychiatric symptoms in Alzheimer's disease. Brain 131:2455–2463.

Brunyé TT, Moran JM, Holmes A, Mahoney CR, Taylor HA. 2017. Non-invasive brain stimulation targeting the right fusiform gyrus selectively increases working memory for faces. Brain Cogn 113:32–39.

Burianova H, McIntosh AR, Grady CL. 2010. A common functional brain network for autobiographical, episodic, and semantic memory retrieval. Neuroimage 49:865–874.

Chang C, Glover GH. 2009. Effects of model-based physiological noise correction on default mode network anti-correlations and correlations. Neuroimage 47:1448–1459.

Chen Y, Chen K, Ding J, Zhang Y, Yang Q, Lv Y, Guo Q, Han Z. 2017. Brain Network for the Core Deficits of Semantic Dementia: A Neural Network Connectivity-Behavior Mapping Study. Front Hum Neurosci 11:267.

Craddock RC, James GA, Holtzheimer PE 3rd, Hu XP, Mayberg HS. 2012. A whole brain fMRI atlas generated via spatially constrained spectral clustering. Hum Brain Mapp 33:1914–1928.

Dermody N, Wong S, Ahmed R, Piguet O, Hodges JR, Irish M. 2016. Uncovering the Neural Bases of Cognitive and Affective Empathy Deficits in Alzheimer's Disease and the Behavioral-Variant of Frontotemporal Dementia. J Alzheimers Dis 53:801–816.

Ding J, Chen K, Chen Y, Fang Y, Yang Q, Lv Y, Lin N, Bi Y, Guo Q, Han Z. 2016. The Left Fusiform Gyrus is a Critical Region Contributing to the Core Behavioral Profile of Semantic Dementia. Front Hum Neurosci 10:215.

Farb NAS, Grady CL, Strother S, Tang-Wai DF, Masellis M, Black S, Freedman M, Pollock BG, Campbell KL, Hasher L, Chow TW. 2013. Abnormal network connectivity in frontotemporal dementia: evidence for prefrontal isolation. Cortex 49:1856–1873.

Fernández-Matarrubia M, Matías-Guiu JA, Cabrera-Martín MN, Moreno-Ramos T, Valles-Salgado M, Carreras JL, Matías-Guiu J. 2018. Different apathy clinical profile and neural correlates in behavioral variant frontotemporal dementia and Alzheimer's disease. Int J Geriatr Psychiatry 33:141–150.

Fox MD, Raichle ME. 2007. Spontaneous fluctuations in brain activity observed with functional magnetic resonance imaging. Nat Rev Neurosci 8:700–711.

Gorno-Tempini ML, Hillis AE, Weintraub S, Kertesz A, Mendez M, Cappa SF, Ogar JM, Rohrer JD, Black S, Boeve BF, Manes F, Dronkers NF, Vandenberghe R, Rascovsky K, Patterson K, Miller BL, Knopman DS, Hodges JR, Mesulam MM, Grossman M. 2011. Classification of primary progressive aphasia and its variants. Neurology 76:1006–1014.

Grieder M, Crinelli RM, Jann K, Federspiel A, Wirth M, Koenig T, Stein M, Wahlund L-O, Dierks T. 2013.

Correlation between topographic N400 anomalies and reduced cerebral blood flow in the anterior temporal lobes of patients with dementia. J Alzheimers Dis 36:711–731.

Guo CC, Gorno-Tempini ML, Gesierich B, Henry M, Trujillo A, Shany-Ur T, Jovicich J, Robinson SD, Kramer JH, Rankin KP, Miller BL, Seeley WW. 2013. Anterior temporal lobe degeneration produces widespread network-driven dysfunction. Brain 136:2979–2991.

Hodges JR, Patterson K. 2007. Semantic dementia: a unique clinicopathological syndrome. Lancet Neurol 6:1004–1014.

Hurley RS, Bonakdarpour B, Wang X, Mesulam M-M. 2015. Asymmetric connectivity between the anterior temporal lobe and the language network. J Cogn Neurosci 27:464–473.

Jobard G, Crivello F, Tzourio-Mazoyer N. 2003. Evaluation of the dual route theory of reading: a metanalysis of 35 neuroimaging studies. Neuroimage 20:693–712.

Kumfor F, Landin-Romero R, Devenney E, Hutchings R, Grasso R, Hodges JR, Piguet O. 2016. On the right side? A longitudinal study of left- versus right-lateralized semantic dementia. Brain 139:986–998.

La Joie R, Landeau B, Perrotin A, Bejanin A, Egret S, Pélerin A, Mézenge F, Belliard S, de La Sayette V, Eustache F, Desgranges B, Chételat G. 2014. Intrinsic connectivity identifies the hippocampus as a main crossroad between Alzheimer's and semantic dementia-targeted networks. Neuron 81:1417–1428.

Landin-Romero R, Tan R, Hodges JR, Kumfor F. 2016. An update on semantic dementia: genetics, imaging, and pathology. Alzheimers Res Ther 8:52.

Liu J, Zhang X, Yu C, Duan Y, Zhuo J, Cui Y, Liu B, Li K, Jiang T, Liu Y. 2016. Impaired Parahippocampus Connectivity in Mild Cognitive Impairment and Alzheimer's Disease. J Alzheimers Dis 49:1051–1064.

Luck D, Danion J-M, Marrer C, Pham B-T, Gounot D, Foucher J. 2010. The right parahippocampal gyrus contributes to the formation and maintenance of bound information in working memory. Brain Cogn 72:255–263.

Mascali D, DiNuzzo M, Serra L, Mangia S, Maraviglia B, Bozzali M, Giove F. 2018. Disruption of Semantic Network in Mild Alzheimer's Disease Revealed by Resting-State fMRI. Neuroscience 371:38–48.

McClelland JL, Rogers TT. 2003. The parallel distributed processing approach to semantic cognition. Nat Rev Neurosci 4:310–322.

McDonough IM, Nashiro K. 2014. Network complexity as a measure of information processing across resting-state networks: evidence from the Human Connectome Project. Front Hum Neurosci 8:409.

Mesulam M-M, Thompson CK, Weintraub S, Rogalski EJ. 2015. The Wernicke conundrum and the anatomy of language comprehension in primary progressive aphasia. Brain 138:2423–2437.

Mummery CJ, Patterson K, Price CJ, Ashburner J, Frackowiak RS, Hodges JR. 2000. A voxel-based morphometry study of semantic dementia: relationship between temporal lobe atrophy and semantic memory. Ann Neurol 47:36–45.

Murphy K, Fox MD. 2017. Towards a consensus regarding global signal regression for resting state functional connectivity MRI. Neuroimage 154:169–173.

Neary D, Snowden JS, Gustafson L, Passant U, Stuss D, Black S, Freedman M, Kertesz A, Robert PH, Albert M, Boone K, Miller BL, Cummings J, Benson DF. 1998. Frontotemporal lobar degeneration: a consensus on clinical diagnostic criteria. Neurology 51:1546–1554.

Nilakantan AS, Voss JL, Weintraub S, Mesulam M-M, Rogalski EJ. 2017. Selective verbal recognition memory

impairments are associated with atrophy of the language network in non-semantic variants of primary progressive aphasia. Neuropsychologia 100:10–17.

Orban P, Dansereau C, Desbois L, Mongeau-Pérusse V, Giguère C-É, Nguyen H, Mendrek A, Stip E, Bellec P. 2018. Multisite generalizability of schizophrenia diagnosis classification based on functional brain connectivity. Schizophr Res 192:167–171.

Owen AM, Milner B, Petrides M, Evans AC. 1996. A specific role for the right parahippocampal gyrus in the retrieval of object-location: a positron emission tomography study. J Cogn Neurosci 8:588–602.

Patterson K, Nestor PJ, Rogers TT. 2007. Where do you know what you know? The representation of semantic knowledge in the human brain. Nat Rev Neurosci 8:976–987.

Power JD, Barnes KA, Snyder AZ, Schlaggar BL, Petersen SE. 2012. Spurious but systematic correlations in functional connectivity MRI networks arise from subject motion. Neuroimage 59:2142–2154.

Power JD, Mitra A, Laumann TO, Snyder AZ, Schlaggar BL, Petersen SE. 2014. Methods to detect, characterize, and remove motion artifact in resting state fMRI. Neuroimage 84:320–341.

Rangarajan V, Hermes D, Foster BL, Weiner KS, Jacques C, Grill-Spector K, Parvizi J. 2014. Electrical stimulation of the left and right human fusiform gyrus causes different effects in conscious face perception. J Neurosci 34:12828–12836.

Reijmer YD, Leemans A, Caeyenberghs K, Heringa SM, Koek HL, Biessels GJ, Utrecht Vascular Cognitive Impairment Study Group. 2013. Disruption of cerebral networks and cognitive impairment in Alzheimer disease. Neurology 80:1370–1377.

Seeley WW, Crawford RK, Zhou J, Miller BL, Greicius MD. 2009. Neurodegenerative diseases target large-scale human brain networks. Neuron 62:42–52.

Shtyrov Y, Pulvermüller F. 2007. Early MEG activation dynamics in the left temporal and inferior frontal cortex reflect semantic context integration. J Cogn Neurosci 19:1633–1642.

Smith SM, Vidaurre D, Beckmann CF, Glasser MF, Jenkinson M, Miller KL, Nichols TE, Robinson EC, Salimi-Khorshidi G, Woolrich MW, Barch DM, Uğurbil K, Van Essen DC. 2013. Functional connectomics from resting-state fMRI. Trends Cogn Sci 17:666–682.

Sormaz M, Jefferies E, Bernhardt BC, Karapanagiotidis T, Mollo G, Bernasconi N, Bernasconi A, Hartley T, Smallwood J. 2017. Knowing what from where: Hippocampal connectivity with temporoparietal cortex at rest is linked to individual differences in semantic and topographic memory. Neuroimage 152:400–410.

Tahmasian M, Pasquini L, Scherr M, Meng C, Förster S, Mulej Bratec S, Shi K, Yakushev I, Schwaiger M, Grimmer T, Diehl-Schmid J, Riedl V, Sorg C, Drzezga A. 2015. The lower hippocampus global connectivity, the higher its local metabolism in Alzheimer disease. Neurology 84:1956–1963.

Tijms BM, Yeung HM, Sikkes SAM, Möller C, Smits LL, Stam CJ, Scheltens P, van der Flier WM, Barkhof F. 2014. Single-subject gray matter graph properties and their relationship with cognitive impairment in early- and late-onset Alzheimer's disease. Brain Connect 4:337–346.

Tondelli M, Wilcock GK, Nichelli P, De Jager CA, Jenkinson M, Zamboni G. 2012. Structural MRI changes detectable up to ten years before clinical Alzheimer's disease. Neurobiol Aging 33:825.e25–36.

Villain N, Fouquet M, Baron J-C, Mézenge F, Landeau B, de La Sayette V, Viader F, Eustache F, Desgranges B, Chételat G. 2010. Sequential relationships between grey matter and white matter atrophy and brain metabolic abnormalities in early Alzheimer's disease. Brain 133:3301–3314.

Vogel A, Gade A, Stokholm J, Waldemar G. 2005. Semantic memory impairment in the earliest phases of Alzheimer's disease. Dement Geriatr Cogn Disord 19:75–81.

Wang J, Zuo X, Dai Z, Xia M, Zhao Z, Zhao X, Jia J, Han Y, He Y. 2013. Disrupted functional brain connectome in individuals at risk for Alzheimer's disease. Biol Psychiatry 73:472–481.

Wang L, Zang Y, He Y, Liang M, Zhang X, Tian L, Wu T, Jiang T, Li K. 2006. Changes in hippocampal connectivity in the early stages of Alzheimer's disease: evidence from resting state fMRI. Neuroimage 31:496–504.

Wirth M, Horn H, Koenig T, Razafimandimby A, Stein M, Mueller T, Federspiel A, Meier B, Dierks T, Strik W. 2008. The early context effect reflects activity in the temporo-prefrontal semantic system: evidence from electrical neuroimaging of abstract and concrete word reading. Neuroimage 42:423–436.

Figures

Figure 1

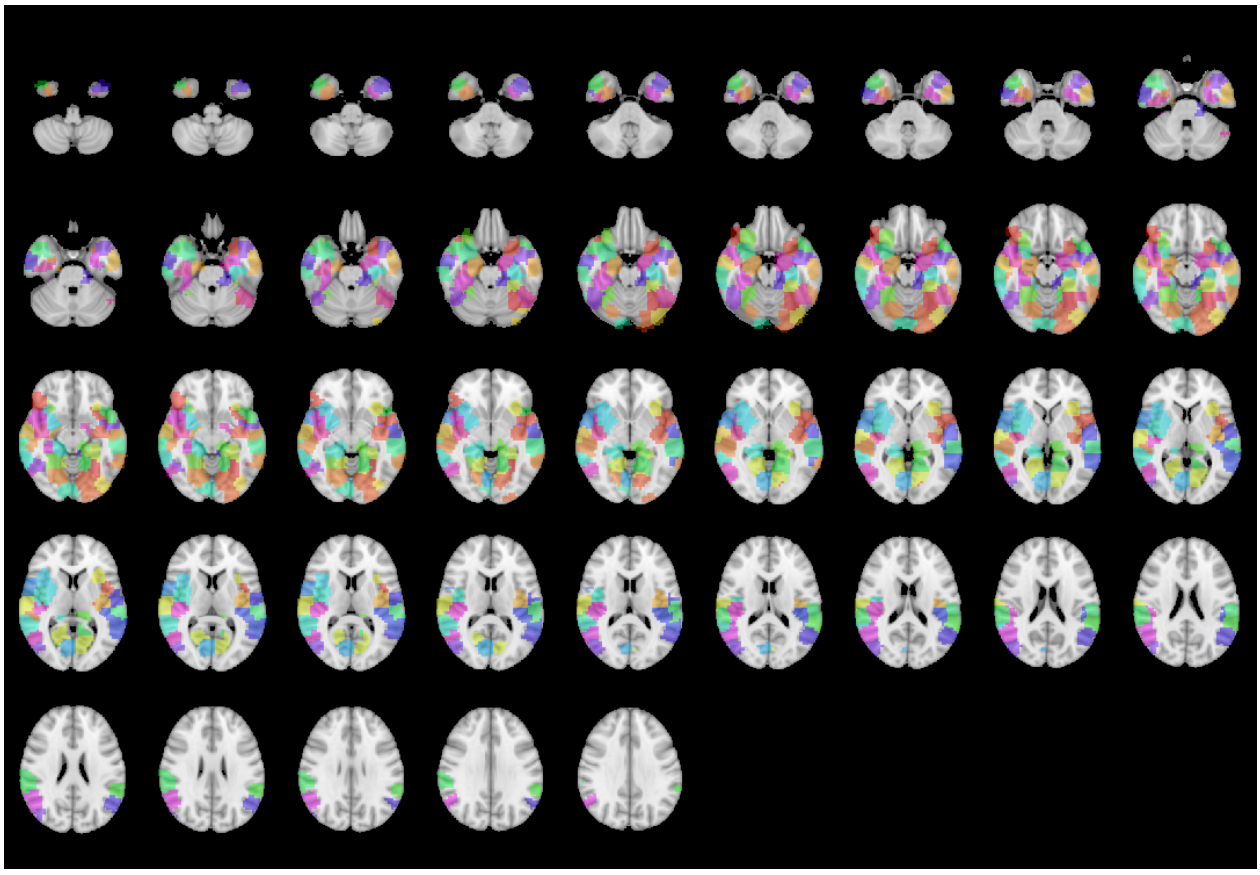

Figure 1. Sixty six nodes from a functional parcellation from the Craddock (2012) atlas (*k* = 200) that were selected based on their overlap with structures in the temporal cortex and the hippocampus.

Figure 2

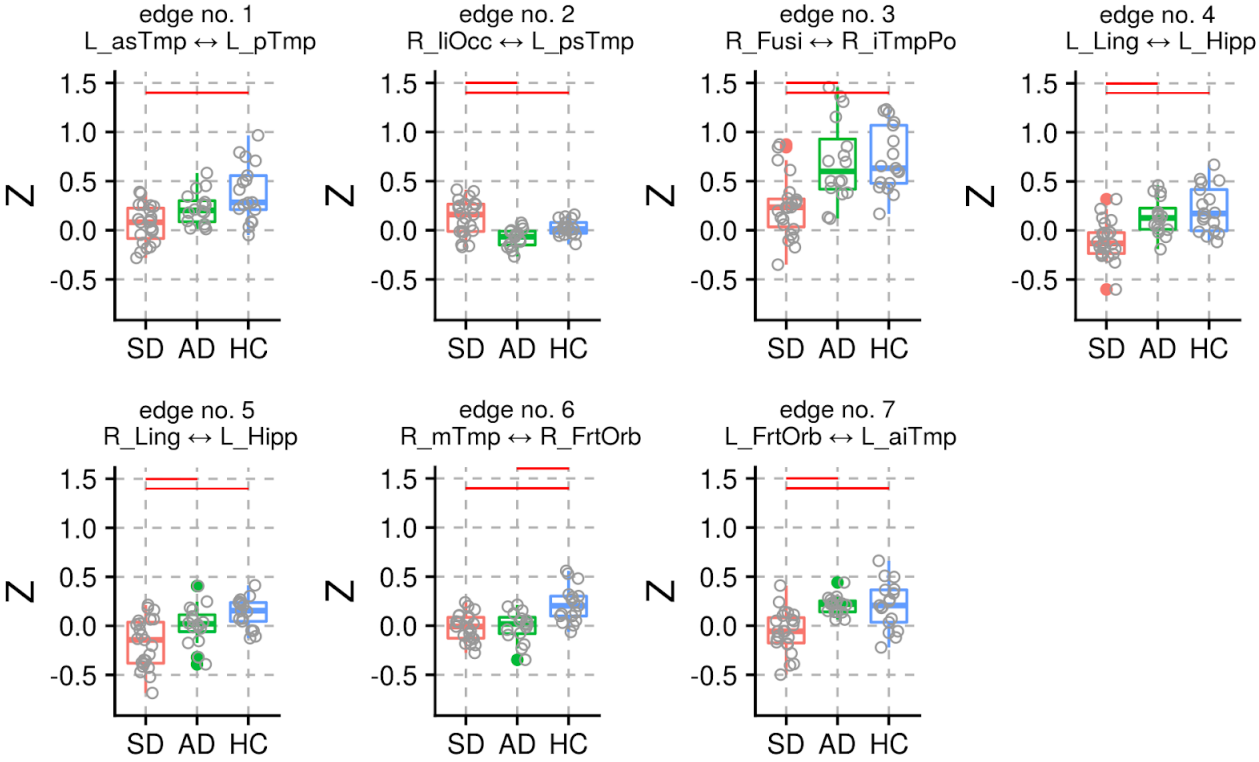

Figure 2: Z-scores of seven connections (edges 1–7) with significant group differences. Post-hoc tests between the three groups were performed, and significant group differences are denoted with red horizontal lines (see also Table 3).

Figure 3

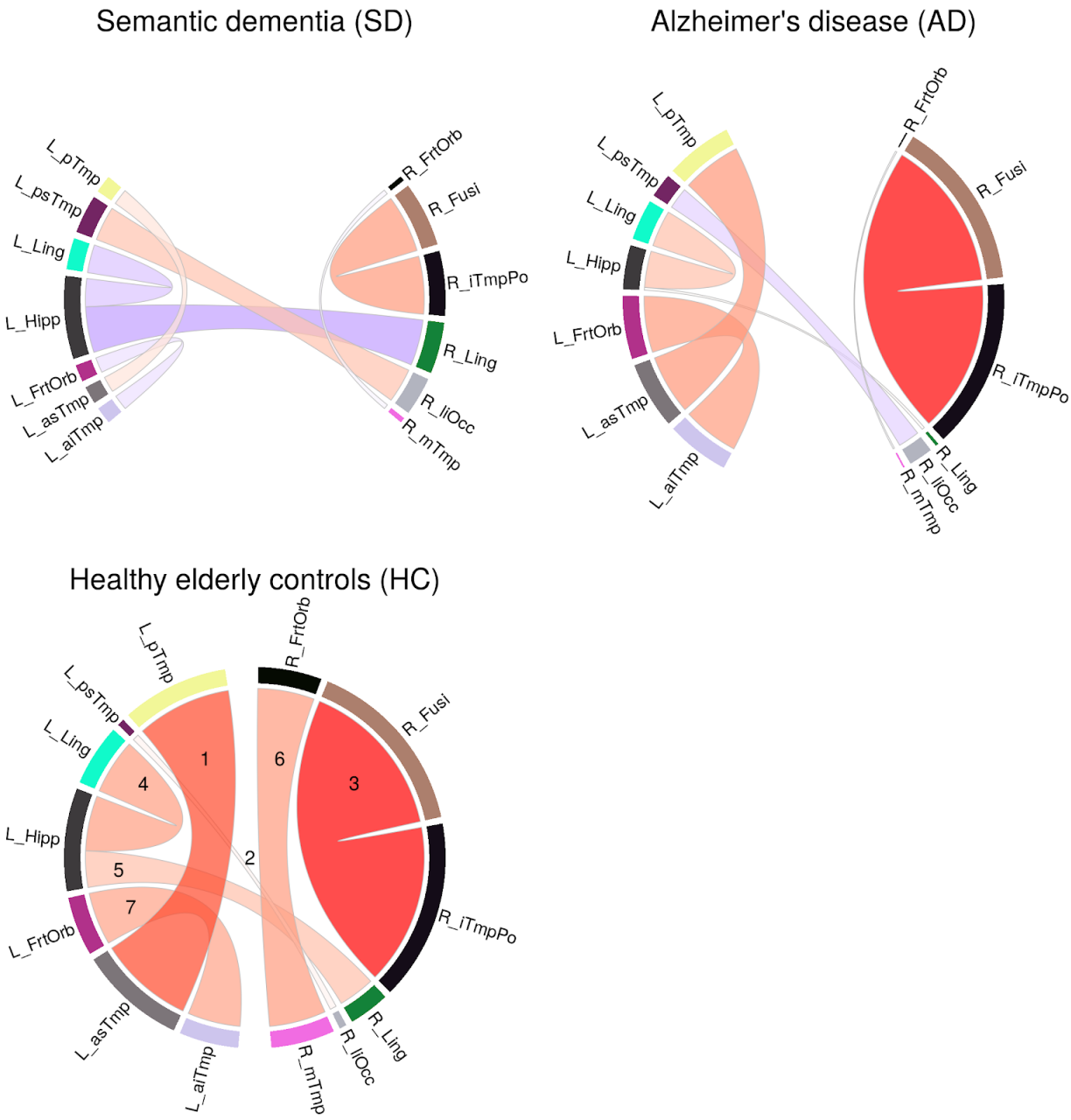

Figure 3: Functional connectivity (FC) strengths (Z-values) of the three groups. Color shades and thickness of the links are proportional to FC strengths, shades of red reflect positive, shades of blue negative strengths. Numbers in HC group indicate edge numbers (see Table 3 for a detailed description of the regions).

Tables

Table 1

Table 1. Descriptives and clinical scores. The non-parametric Kruskal-Wallis-Test was run to assess statistically relevant differences over all three groups (not depicted in the table). All clinical scores that were available for all three groups (i.e. MMSE, BNT, AF, VF) yielded a *p*-value below 0.001. A significant age effect was found ($p < 0.01$), but no effect of education. Group-wise post-hoc comparisons were performed using the non-parametric Kolmogorov-Smirnov-Test. Note that in the SD group, education and neuropsychological test scores were only available from the Stockholm site (statistics in italics).

	HC (n=17)	**AD (n=16)**	**SD (n=23; *n=5*)**	**HC-AD**	**HC-SD**	**AD-SD**
	Mean (SD)	**Mean (SD)**	**Mean (SD)**	**p-value**	**p-value**	**p-value**
Age, years	69.5 (3.4)	69.6 (8.5)	61.8 (7.6)	n.s.	< 0.01	n.s.
Gender (F:M)	12:5	7:9	10:13	-	-	-
Education, years	13.9 (3.1)	13.1 (3.0)	*12.4 (1.5)*	n.s.	*n.s.*	*n.s.*
CDS	-	1.0 (1.0)	*1.8 (2.2)*	-	-	*n.s.*
GDS	-	2.9 (0.7)	*3.8 (0.4)*	-	-	*n.s.*
MMSE (max 30)	28.8 (0.8)	24.5 (4.8)	*21.4 (5.5)*	< 0.01	*< 0.01*	*n.s.*
BNT (max 60)	54.4 (3.7)	45.6 (6.5)	*8.2 (5.7)*	< 0.01	*< 0.01*	*< 0.01*
AF, animals/minute	23.8 (5.9)	14.1 (4.2)	*5.6 (4.3)*	< 0.001	*< 0.01*	*< 0.01*
VF, verbs/minute	21.9 (5.8)	11.9 (5.0)	*7.0 (2.8)*	< 0.01	*< 0.01*	*n.s.*

Table 2

Table 2. Seven functional connections that demonstrated significant group differences. Connections are sorted according their F-value.

Edge no.	Node no.	Node no.	Region	Region	*F*-value	FDR adj. *p*-value
4	70	37	Left lingual gyrus / intracalcarine cortex / precuneous cortex	Left hippocampus / thalamus	12.94	0.030
3	198	32	Right fusiform cortex / parahippocampal gyrus	Right inferior temporal pole	12.41	0.030
6	153	71	Right anterior middle temporal gyrus / superior temporal gyrus	Right orbitofrontal cortex	12.27	0.030
7	112	72	Left orbitofrontal cortex / insular cortex	Left anterior inferior temporal gyrus / middle temporal gyrus	11.88	0.030
2	85	24	Right lateral inferior occipital cortex / lateral superior occipital cortex	Left posterior superior temporal gyrus / central opercular cortex / parietal opercular cortex / planum temporale	11.3	0.035
1	129	11	Left anterior superior temporal gyrus / middle temporal gyrus / insular cortex	Left posterior middle temporal gyrus / superior temporal gyrus	11.05	0.035
5	89	37	Right lingual gyrus / intracalcarine cortex	Left hippocampus / thalamus	10.74	0.038

Table 3

Table 3. Post-hoc Tukey HSD *p*-values for the three combination of group levels (rows) and for each of the seven node-pairs that had a significant group effect (columns). Significant values reflect the group effect was driven by a specific group level contrast. Lowest *p*-value per edge highlighted in bold.

Edge No.	1	2	3	4	5	6	7
AD vs HC	0.098	0.082	0.979	0.538	0.217	**0.001***	0.997
SD vs AD	0.064	**<0.001***	**<0.001***	0.002*	0.024*	0.975	**<0.001***
SD vs HC	**<0.001***	0.044*	**<0.001***	**<0.001***	**<0.001***	**<0.001***	**<0.001***